ARTICLE

OBC
www.rsc.org/obc

Self-organization of lactates in the gas phase

Nicole Borho and Martin A. Suhm *
Institut für Physikalische Chemie, Universität Göttingen, Tammannstr. 6, D-37077, Göttingen, Germany

Received 25th July 2003, Accepted 10th October 2003
First published as an Advance Article on the web 27th October 2003

Chiral recognition and subsequent selective self-organisation into hydrogen-bonded *n*-mers is observed in supersonic methyl lactate expansions. The ν_{OH} and $\nu_{C=O}$-vibrations are investigated by *ragout*-jet FTIR-spectroscopy and lead to the assignment of homo- and heterochiral clusters of at least three different cluster sizes. Whereas homo- and heterochiral dimers are formed in similar amounts in the racemic mixture, prominent absorptions due to different homochiral and heterochiral lactate trimers and tetramers indicate highly specific chiral self-recognition beyond molecular pairs. Chemical modification of the ester-group (methyl-, ethyl- and isopropyl-lactate) and argon admixture to the helium expansion contribute importantly to an understanding of the cluster spectra and topology.

1 Introduction

Chiral recognition is an essential ingredient of most biomolecular processes. In the timeless lock-and-key metaphor proposed by E. Fischer,[1] the mirror copy of a chiral key will not fit a given chiral lock as well as the original key. By symmetrizing the problem, one arrives at the phenomenon of chiral self-recognition, which is best visualized by the disparate handshakes between left and/or right hands.[2,3] At the level of molecules, a (homochiral) complex between two identical chiral molecules is dissimilar from (and diastereomeric to) that between one of these molecules and its mirror copy (heterochiral complex). A detailed understanding of this kind of chiral discrimination in molecular complexes requires the study of the underlying intermolecular forces,[4,5] *i.e.* repulsive and attractive van der Waals interactions and most importantly hydrogen bonding. These intermolecular forces are accessible to quantum chemical calculations of increasing sophistication.[6,7] Once a chiral element is present in a molecule, achiral substituents can amplify chiral recognition in favourable cases.[8]

In the search for realistic, yet simple model systems for chiral self-recognition, several aspects deserve attention. More than one functional group should be present in the molecule to establish multiple contacts. For topological simplicity, groups which can act as hydrogen bond donors *and* acceptors should be used sparingly. On the other hand, they allow for hydrogen bond cooperativity, an important ingredient in biochemical recognition. Intramolecular hydrogen bonding should compete with intermolecular interactions to model biochemical encounters in solution, *i.e.* out of a solvated state. Here, we explore the aggregation of lactates, $CH_3CH(OH)COOR$, which combine several functional groups, intramolecular hydrogen bonding, and chirality. Their simplicity enables both detailed gas phase studies and high-level quantum chemical treatments—two prerequisites for an understanding which goes beyond the levels accessible to biochemical phenomena themselves.

By reducing the model system to a compact molecule with only three functional groups capable of medium-sized intermolecular interactions (OH, C=O, ORR′), the steric and electronic constraints may be too subtle to lead to significant chiral discrimination in a molecular complex. One way of circumventing this danger is to introduce a metal cation to which the chiral molecules are coordinated as ligands. Such coordination centers amplify the chiral recognition due to the strength of ion–dipole interactions. It is thus not surprising that impressive and quite elementary cases of chiral self-recognition have been found in coordination compounds.[9,3,10] X-Ray diffraction is the method of choice for the study of such systems and both bi- and tri-centric examples have been observed. In each case, there is a strong preference for homochiral complexes, possibly a consequence of the central ion coordination geometry. A similar enhancement of chiral recognition can be observed in charged clusters, such as in protonated serine octamers,[11,12] which have even been linked to the phenomenon of biomolecular homochirality.[13]

Our goal is to detect more subtle and even more simple examples of molecular handshakes, which do not require the help of a surplus charge. As a consequence, lifetime and stability in solution are limited and cold supersonic gas phase expansions are better suited to generate them. Crystallography and mass spectrometry have to be replaced by spectroscopy for detection and the structural conclusions are necessarily more indirect. However, in contrast to the situation in solution which is plagued by thermal and conformational broadening of the spectra,[14] IR-spectroscopy in supersonic jets is sensitive enough to detect subtle recognition effects and the connection to electronic structure theory is as direct as it can be.

The pioneering work in supersonic jet spectroscopy of chiral molecular complexes is due to Zehnacker *et al.*[15–18] using laser-induced fluorescence (LIF) and Giardini-Guidoni *et al.* performing resonance-enhanced multiphoton ionization (REMPI) in combination with time-of-flight mass spectrometry.[19–21] An advantage of these highly sensitive techniques is their ability to quantify binding energy effects and to allow for conformational selection. However, both techniques typically require an aromatic chromophore, which complicates the interactions and their theoretical modelling, in particular for homodimers (*i.e.* dimers built from two constitutionally identical monomer units, irrespective of their chirality). Therefore, no cases of chiral self-recognition have been studied by these techniques so far. High-resolution microwave jet spectroscopy can provide detailed structural and electronic information of diastereomeric complexes such as moments of inertia and dipole moments. However, the spectroscopic assignment is not a trivial task and up to now, only one heterochiral dimer of 2-butanol has been assigned by Howard and King.[22,23] *Ragout*-jet FTIR-spectroscopy[24,25] offers an alternative and very efficient means of detecting chiral recognition phenomena in the gas phase for sufficiently volatile compounds. It is our method of choice, as it has no other constraints such as the existence of aromatic chromophores or non-vanishing dipole moments. However, it can clearly profit from subsequent studies by the other spectroscopic techniques, as it only provides indirect cluster size and structural information.

Our *ragout*-jet FTIR studies of chiral self-recognition in 2-butanol[26] and glycidol[2,27] revealed the importance of

DOI: 10.1039/b308580e

conformational simplicity and of more than one functional group in the monomer in order to establish a well-defined molecular handshake. The investigation of α-hydroxy-esters like methyl lactate (MLac) with their three (hydroxy-, carbonyl-, and alkoxy-) functional groups represents a natural continuation of this strategy. While it has more conformational degrees of freedom than glycidol, MLac at room temperature in its monomeric form is predicted to exist almost exclusively (>90%) in the hydrogen-bonded (*syn*-*syn*) conformation.[28,29] Detailed matrix-isolation and quantum chemical studies of the related compounds methyl glycolate and methyl α-hydroxy-isobutyrate confirm that 92% and 88% of the monomers adopt *syn*-*syn* conformations,[30–32] respectively. MLac was studied before by IR-spectroscopy in the neat liquid,[33,34] in matrix isolation,[35] and in dilute CCl_4 solution.[33,36,29] In solution, emphasis was often put on vibrational circular dichroism.[36,28,29,37,38]

Some evidence for condensed phase chiral recognition effects in MLac and its derivatives has been reported. The mixing enthalpy of *R*- and *S*-MLac is + 14.2 J mol^{-1} at 298 K, indicative of a slight preference for homochiral interactions.[39] Quite spectacular differences in the boiling points of racemic and enantiopure trifluorolactates have been found,[40,41] but are claimed to be specific to the fluorinated compounds. Less surprisingly, highly enantioselective inclusion of MLac and ethyl lactate (ELac) in a dipeptide has been reported.[42] Thus, MLac and its derivatives appear to be interesting, yet simple prototypes in the field of molecular recognition.

In this work, we present unambiguous IR-spectroscopic evidence for strong chiral recognition in isolated multimeric aggregates of MLac and its higher ester homologues. This study represents a first step in our effort to understand the pronounced selectivity in the self-aggregation of α-hydroxy-carbonyl compounds at the molecular level.

2 Experimental

The infrared spectra were obtained using *ragout*-jet FTIR-spectroscopy which has been described in detail in Ref. 24. The method is based on the synchronisation of giant gas pulses to complete rapid mirror scans, generating one broad-band FTIR spectrum per pulse. The OH-stretching (carbonyl-stretching) spectra were recorded by a Bruker IFS 66v/S spectrometer equipped with an InSb (MCT)-detector, CaF_2(KBr)-beam-splitter and a 2.5–3.5 μm (4.4–9.1 μm) optical filter at 2 cm^{-1} resolution.

The giant gas pulses were realized *via* a pneumatically operated slit nozzle of 120 mm length and 0.4–0.5 mm width. Flow rates of 1.3 mol s^{-1}, gas pulses in excess of 0.14 s and repetition rates up to 0.1 Hz were accessible using a large buffer volume of 15 m^3 in combination with a series of roots pumps. Substance volume fractions of 0.03–0.1% in the carrier gas (pure He or Ar/He-mixtures) were realized using a saturator at variable temperatures. Differences in stagnation pressure scaling of the absorptions are taken as strong evidence for different cluster sizes. A 10 × 20 mm section of the collimated IR beam crossed the expansion 16 mm downstream of the nozzle.

The chiral self-recognition effect is revealed by spectral comparison of the racemate and one enantiomer of a chiral compound under identical experimental conditions, including saturator temperature and volume. The high reproducibility and baseline stability of broad-band FTIR-spectrometers allows for the implementation of sensitive difference techniques. The observed deviation in the lactate volume fraction of racemic and enantiopure gas mixtures was typically <5% (≈20% for ELac due to a difference in liquid levels in the saturator). The fact that the gas phase spectra of racemic and enantiopure compounds are indistinguishable provides evidence for the absence of significant volatile impurities. Differences in the jet spectra can thus only be due to diastereomeric cluster formation.

S-(−)-MLac (>97% purity), rac. MLac (>99%), *R*-(+)-ELac (>99%) and *S*-(−)-isopropyl lactate (ILac) (>98%) were obtained from Fluka, *S*-(−)-ELac (>99%) from Merck. All compounds were used without further purification. In the case of ELac, the *S*-(−)-enantiomer and the 1 : 1-mixture of both enantiomers were measured.

3 Results and discussion

3.1 Methyl lactate

The cold supersonic jet spectra in the OH-stretching range of 0.09% enantiopure *S*-(−)-MLac in He at 1.0 bar (trace b)) and 0.6 bar stagnation pressure (trace c)) are presented in Fig. 1. Analogous results were obtained for a stagnation pressure of 1.4 bar (not shown). Several sharp and some broader bands can be observed, the strongest of which are labeled M, D, T, Q and C. The labeling is inspired by differences in pressure dependence, which we interpret as being due to different cluster sizes. This is underlined by trace d), which is the difference b) − 1.45 × c), scaled to equal D band absorption. Negative bands in the difference spectrum are thought to be due to smaller units, whereas bands pointing into the positive direction are due to larger clusters. There is only one prominent negative band (M), the center of which is 10 cm^{-1} red-shifted relative to the room temperature gas phase spectrum of the monomer (see trace a)). This is typical for an internally hydrogen-bonded conformation due to thermal weakening and consistent with the soft slope of the band shape to higher wavenumber. It is also consistent with *ab initio* predictions[37,29,28] of a single important, internally hydrogen-bonded conformation. Therefore, we can unambiguously identify the M band with the dominant monomer conformation and we can tentatively assign the D bands at 3545, 3527, 3515, and 3496 cm^{-1} (Da, Db, Dd, and De) to dimers. While these bands show a very similar pressure dependence, we

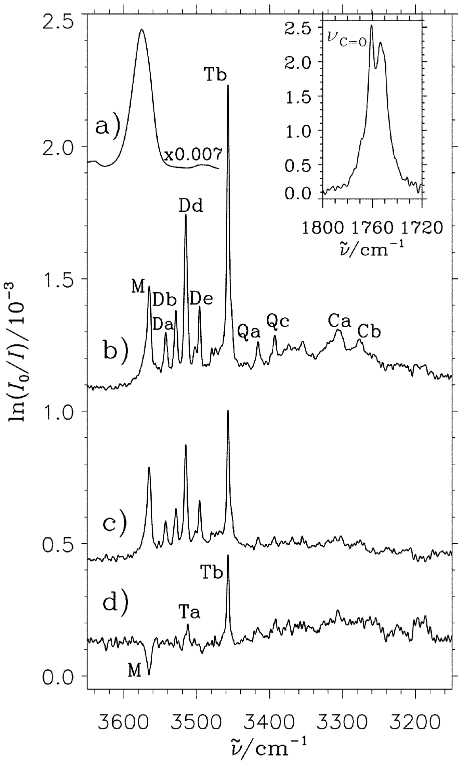

Fig. 1 *Ragout*-jet FTIR-spectra of enantiopure methyl lactate (MLac, 0.09% in He) at b) 1.0 bar and c) 0.6 bar stagnation pressure, each based on 200 gas pulses of 0.14 s duration (1.5 h measurement time). The difference spectrum d) = b) − 1.45 × a) removes Da–De absorptions. The 298 K gas phase O–H stretching band of the monomer is shown in trace a) (0.08% MLac in He, *p* = 744 mbar, optical path length = 334 mm). The $\nu_{C=O}$ absorption corresponding to spectrum b) is inserted in the upper right corner.

Table 1 OH-stretching band maxima in cm^{-1} for racemic (rac.) and enantiopure (en.) MLac in He expansions (Figs. 1 and 2) with assignment of heterochiral (het) and homochiral (hom) character and tentative cluster size assignment n

Size	Label	rac.	en.	Assignment
$n = 1$	M	3565	3565	—
$n = 2$	Da	3543	3543	hom+het
$n = 2$	Db	—	3529	hom
$n = 2$	Dc	3527	—	het
$n = 2$	Dd	3515	3515	hom
$n > 2$	Ta	—	3512	hom
$n = 2$	De	3496	3496	hom
$n = 2$	Df	3467	—	het
$n > 2$	Tb	3457	3457	hom
$n > 2$	Tc	3443	—	het
$n \gg 2$	Qa	—	3416	hom
$n \gg 2$	Qb	3401	—	het
$n \gg 2$	Qc	—	3393	hom
$n \gg 2$	Qd	3354	—	het
$n \gg 2$	Ca	—	3306	hom
$n \gg 2$	Cb	—	3279	hom

cannot rigorously exclude trimer contributions in some of them, based on our previous experience with neighboring cluster sizes.[43] The Tb band and the Q and C bands correspond to clusters beyond dimers. The difference in pressure scaling for Tb is substantial. Also, a small T component underneath Dd is revealed. This Ta band is red-shifted by ≈3 cm^{-1} with respect to Dd. Small bands to the right of Tb (Qa and Qc) show an even stronger pressure dependence. The broad and strongly red-shifted absorptions Ca and Cb are indicative of a cooperative OH bond pattern in larger clusters. The classification obtained from the scaling procedure is listed in Table 1 together with the positions of the observed band maxima.

Important clues can be drawn from the C=O stretching region. The C=O stretching vibration of MLac clusters recorded under the same experimental conditions as trace b) is inserted in Fig. 1. The main cluster absorption (1754 cm^{-1}) is slightly red-shifted with respect to the band center of monomer absorption in the gas phase (1755 cm^{-1}), but additionally a sharp blue-shifted band appears at 1760 cm^{-1}. The latter increases with pressure and can thus be attributed to the same clusters as the Tb or C bands. A slight red-shift with respect to the intramolecularly bound monomer is easily rationalized for an intermolecular O–H ··· O=C band, as dipolar field effects[33] may be reduced in the latter. A blue-shift is consistent with more or less free (or C–H coordinated) carbonyl groups, along with the emergence of cooperative O–H ··· O–H bonds.

Hence, a plausible interpretation of the enantiopure MLac cluster expansion based on Fig. 1 is the following: A single, internally hydrogen-bonded monomer conformation (M), several hydrogen-bonded dimer conformations (D), and at least two different, larger cluster sizes with cooperative hydrogen bond elements (T, Q, C) appear in the homochiral spectrum.

Fig. 2 displays spectra of racemic MLac under experimental conditions equivalent to those of the enantiopure compound in Fig. 1. Here, homochiral cluster absorptions are partially replaced by those of heterochiral clusters, *i.e.* clusters assembled from monomer units of different handedness. This explains the higher complexity of the racemate spectra at a) 1.0 bar and b) 0.6 bar stagnation pressure. The homochiral cluster bands Dd, De, Tb, Ca and Cb are reduced in intensity and apparently free of significant overlap with heterochiral cluster absorptions. Db (3529 cm^{-1}) overlaps with a slightly (2 cm^{-1}) red-shifted heterochiral absorption Dc. The purely heterochiral peaks Df and Tc differ in their pressure dependence and are labeled in analogy to the De and Tb peaks, which show a similar evolution with pressure. The pressure dependence of the heterochiral Qb peak outperforms that of the Tc peak (compare traces a) and b) in Fig. 2) and is probably due to an even larger cluster, whereas C bands (and also the sharp blue-shifted C=O stretching band) are hardly visible in the racemate spectrum. This is also confirmed in the D-scaled difference spectrum c), which in addition exhibits a broad, unstructured background absorption due to large clusters. More quantitatively, the normalized intensity increase from 0.6 bar to 1.0 bar amounts to about 1 : 1.3 : 1.7 : 2.1 for M : D : T : Q, whereas it is approximately 1 : 1.5 : 2.1 : 3.0 from 0.6 bar to 1.4 bar. This suggests a smooth increase in cluster size in the sequence M : D : T : Q. However, the broad background absorption from 3550–3200 cm^{-1} renders a more rigorous analysis of integrated band strengths difficult.

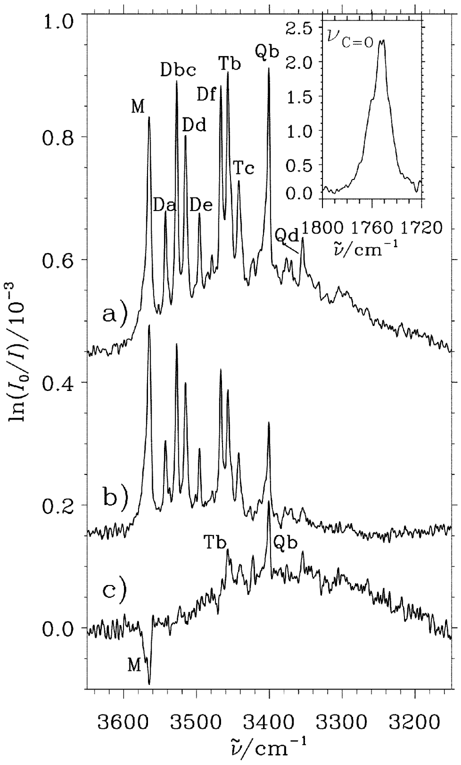

Fig. 2 *Ragout*-jet FTIR-spectra of racemic MLac (0.09% in He, 300 gas pulses) at a) 1.0 bar and b) 0.6 bar. Information on cluster size can be obtained from the difference spectrum c) = a) − 1.39 × b), where Da–Dd cancel. The $\nu_{C=O}$ absorption under the same experimental conditions as in a) is inserted in the upper right corner.

At this point, a statistical analysis of homochiral cluster abundance in the racemic mixture is adequate. Several studies of supersonic jet expansions[44,2] indicate that cluster formation in such expansions is mainly kinetically controlled so that the cluster abundance should mirror at least qualitatively the underlying statistics. Table 2 summarizes the statistical contributions of homo- and heterochiral clusters as a function of size. Homochiral and heterochiral dimers should appear in a 1 : 1 ratio in the racemate, but this equipartition may be obscured by differences in the band strength of the corresponding dimer absorptions. More directly, any homochiral dimer peak should decrease by a factor of two upon dilution in the racemate. This expected twofold racemic dilution factor was confirmed in the case of glycidol[27,2] and has provided an important confirmation of the size assignment as well as evidence for kinetic control of cluster formation in the jet.

Fig. 3 compares corresponding IR spectra of a) racemic and b) enantiopure MLac at 1.0 bar. For the Dd band, the intensity reduction upon racemization is close to twofold, but the Ta contribution to this peak complicates the analysis. De also decreases by a factor of two, whereas Da stays more or less constant. The latter finding points at some heterochiral contribution to Da, similar to the overlap found for Db and Dc. The pure heterochiral dimer spectrum can be obtained by subtracting one half of trace b) from trace a). The resulting spectrum is shown in trace c) and it clearly reveals the heterochiral dimer

Table 2 Statistical distribution of homo- and heterochiral clusters of size n

	$n = 2$	$n = 3$	$n = 4$	n
hom : hom[a]	1 : 2	1 : 4	1 : 8	$1 : 2^{n-1}$
hom : het[b]	1 : 1	1 : 3	1 : 7	$1 : (2^{n-1} - 1)$
hom	*RR*, *SS*	*RRR*, *SSS*	*RRRR*, *SSSS*	2
het[c]	*RS*, *SR*	*RRS*, *SSR*, *RSR* *SRS*, *SRR*, *RSS*	*SRSR*, *RRSS*, *SSRR* *RSSR*, *SRRS*, *RSRS* *RRRS*, *SSSR*, *RSSS* *SRRR*, *SRSS*, *RSRR* *SSRS*, *RRSR*	$2^n - 2$

[a] Concentration ratio of homochiral clusters in the racemate *vs.* the enantiopure expansion. [b] Concentration ratio of homochiral *vs.* heterochiral clusters in the racemate. [c] For $n = 4$, two heterochiral cluster types with $R : S$ ($S : R$) ratios of 1 : 1 or 1 : 3 are possible.

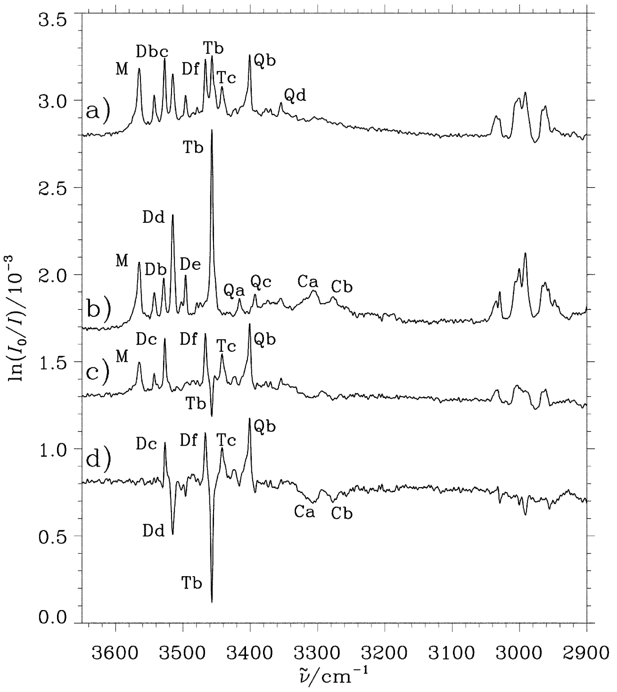

Fig. 3 Chiral recognition in the spectra of MLac. Traces a) and b) correspond to trace a) in Fig. 2 and trace b) in Fig. 1, respectively. c) shows the synthetic heterochiral dimer contributions and corresponds to a) − 0.5 × b). The difference d) = a) − b) represents the fraction of absorption which is sensitive to chirality. Positive bands arise from heterochiral, negative signals from homochiral clusters.

peaks Da, Dc and Df—one peak less than for the homochiral dimer absorptions.

The next peak in the synthetic heterochiral dimer spectrum (Tb) is negative and thus due to a larger cluster, where the dimer statistics do not apply. This peak is about three to four times weaker in the racemic spectrum b) than in the enantiopure spectrum a). According to Table 2, this would point to a trimer origin from a purely statistical viewpoint. However, one has to keep in mind two factors which can systematically reduce the racemic dilution factor. One of them is the effect observed for Da—accidental overlap with a heterochiral peak. The second effect is a departure from kinetic control. Given that Tb is due to a dominant homochiral cluster (see trace b)), it may form at higher than statistical abundance in the racemic mixture. For these two reasons, the observed apparent racemic dilution factor of three to four must be regarded as a lower bound. Thus, it is not inconsistent with a tetramer assignment, although the latter should ideally lead to a dilution factor of eight. Statistically, one would expect a dominance of heterochiral absorptions over homochiral absorptions in the racemic spectrum (3 : 1 for a trimer assignment, 7 : 1 for a tetramer assignment, see Table 2). Even when allowing for some overlap with D bands and for differences in band strength, this is clearly not the case. Some deviation from statistical behavior is thus unavoidable and the Tb signal necessarily reflects a preference for homochiral clusters, whether they are trimers or tetramers. A trimer assignment of Tb implies less drastic deviations from statistical oligomerization and is therefore our preferred assignment in the absence of rigorously size-resolved experiments.

This brings us to the most surprising spectral feature, the Qb band. It scales more strongly with pressure than the T-bands and is therefore assigned to a larger cluster. Its OH-stretching intensity hints at a remarkable chiral recognition effect, as it accounts for at least 80% of the IR absorption in the relevant range. In the C=O stretching range (shown as an inset in Fig. 2), the Qb band correlates with an intensity enhancement on the low frequency side, which indicates that the carbonyl groups are engaged in the aggregation process. If Tb is due to homochiral trimers, Qb might be due to heterochiral tetramers, of which there are 2 types (1 : 1 and 1 : 3 ratio of the enantiomers), having a 38–50% statistical abundance each (see Table 2). The integrated absorption in the Q range of the racemic expansion substantially exceeds that of the enantiopure expansion, supporting the preferred formation of such heterochiral tetramers.

The homochiral Ca and Cb bands must correspond to tetramers or larger clusters, in which cooperative OH ··· OH hydrogen bonding is unstrained and fully developed, like in the corresponding alcohols.

In summary, the supersonic jet spectra of MLac exhibit an impressive amount of chiral discrimination, as evidenced in trace d) of Fig. 3, which shows the difference between a) and b). In the dimer region, several hetero- and homochiral absorptions cancel, but *e.g.* the Dc/Dd pair does not. In the T- and C-regions, homochiral clusters prevail, whereas the Q region is dominated by one type of heterochiral cluster. There is also evidence for chiral discrimination in the C–H stretching region (see Fig. 3), with some sharp bands exclusively in the enantiopure expansion. This indicates that the clusters causing the T or C bands involve a significant change in the C–H environment relative to monomers and dimers, possibly due to involvement of weak C–H hydrogen bonds.

3.2 Admixture of argon

The admixture of Ar to the He-expansion can have two effects, as verified in earlier *ragout*-jet FTIR studies.[24,45,2] It can relax conformational equilibria due to more efficient collisional energy transfer and it can coat the clusters with Ar shells, resulting in a nanomatrix environment. Fig. 4 shows the effect on MLac. Spectra a) (enantiomer) and c) (racemate) are obtained with trace amounts of argon in the He expansion. Relative to the analogous pure He expansions shown in Figs. 1 and 2 (trace a)), small new peaks and shoulders emerge at the origin of the arrows (D@Ar$_n$ at 3486 cm^{-1} and T@Ar$_n$ at 3452 cm^{-1}). These peaks develop into major absorptions at an Ar admixture of *ca.* 2% (traces b) and d)). At the same time, the complicated D band structure collapses almost completely. This indicates that conformational isomerism is reduced by the Ar bombardment and only the most stable conformers survive in the Ar shells. Interestingly, the Tb band appears to survive. Ar condensation

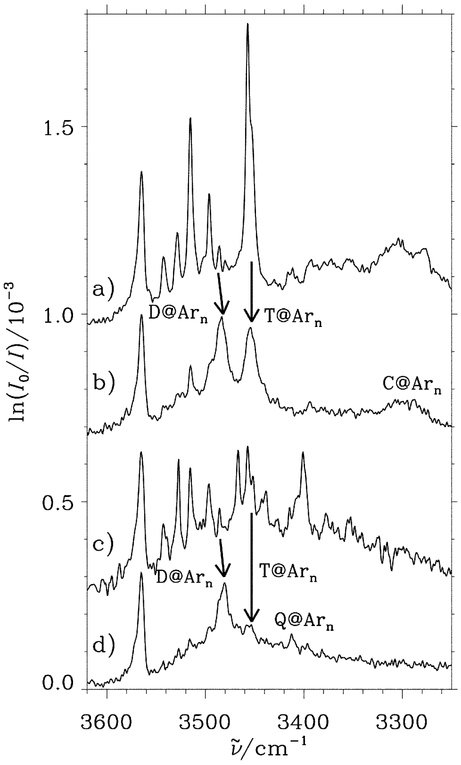

Fig. 4 Argon coating and conformational relaxation. *Ragout*-jet-FTIR-spectra (200 pulses, 0.6–1.0 bar stagnation pressure) of enantiopure MLac a) in He with traces of Ar and b) in ≈2% Ar in He; racemic MLac c) in He with traces of Ar and d) in ≈2% Ar in He.

is quite subtle, as illustrated by the fact that the monomer units survive uncoated, presumably because their dispersion interaction is smaller than that of the clusters and collisional energy can be dissipated less efficiently. Significant Ar-coating of MLac monomers is achieved for 0.1% MLac in 1 : 1 Ar : He mixtures.

The Ar-induced shift of the corresponding MLac bands is instructive. In the D-region, the nanomatrix band appears to lower frequency with respect to most free D-bands, certainly with respect to the center of gravity of these bands. Once formed, the D@Ar$_n$-absorption continues to shift to lower frequencies with increasing Ar concentration. Quite obviously, these dimer structures are relatively open so that the rare gas atoms can interact with their functional groups. Chiral discrimination is much reduced in the coated dimers. In complete contrast, the T@Ar$_n$ bands are only slightly shifted with respect to the corresponding dominant T band and the band position does not evolve noticeably with Ar concentration. Within the available signal-to-noise ratio, the same appears to be true for the weaker absorptions in the Q and C regions. Apparently, the T structure and possibly also the Q and C structures have more protected OH groups. Interestingly, the pronounced chiral recognition effect survives in these Ar-coated clusters. The T@Ar$_n$ and C@Ar$_n$ bands are much stronger in the enantiopure expansion, whereas the weak Q@Ar$_n$ band is somewhat more prominent in the racemic mixture. For T@Ar$_n$, the three- to fourfold racemic dilution factor is approximately confirmed.

The Ar-coating experiment provides a strong confirmation for the earlier M-D-T-Q-C grouping of the individual bands according to their pressure dependence. It shows that chiral discrimination in MLac clusters beyond the dimers is a surprisingly robust phenomenon and it hints at a compact structure of these larger aggregates.

3.3 Ethyl lactate

In the absence of direct structural information from microwave spectroscopy and direct cluster size determination from fragmentation-free mass-selective techniques, we employ chemical substitution to obtain further information on this selective aggregation phenomenon. In the present work, substitution of the methyl ester by more bulky alkyl groups is explored.

Table 3 OH-stretching band maxima in cm^{-1} for racemic and enantiopure ELac in He expansions (Fig. 5) with assignment of heterochiral (het) and homochiral (hom) character

Size	Label	rac.	en.	A
$n = 1$	M	3562	3562	—
$n = 2$	Da	—	3550, 3546	hom
$n = 2$	Dc	3542	—	het
$n = 2$	Db	—	3537, 3533	hom
$n = 2$	Dd	3517	3517	hom
$n = 2$	De	—	3500, 3491	hom
$n > 2$	Tb	—	3457, 3453	hom
$n \gg 2$	Qb	3402	—	het

Fig. 5 displays the OH-stretching spectra and chiral recognition analysis for ELac at 0.6 bar stagnation pressure. In analogy to Fig. 3, trace a) shows the jet spectrum of the 1 : 1 mixture of *R*/*S*-ELac, b) the enantiopure spectrum, c) the synthetic heterochiral dimer spectrum obtained from a) − 0.5 × b) and d) the difference a) − b). The main features of the ELac spectra are very similar to those of MLac, and we therefore label them analogously, adding an E- or M- (or I- for the isopropyl ester, *vide infra*) where distinction is necessary. Table 3 contains the ν_{OH} wavenumbers of spectra a) and b).

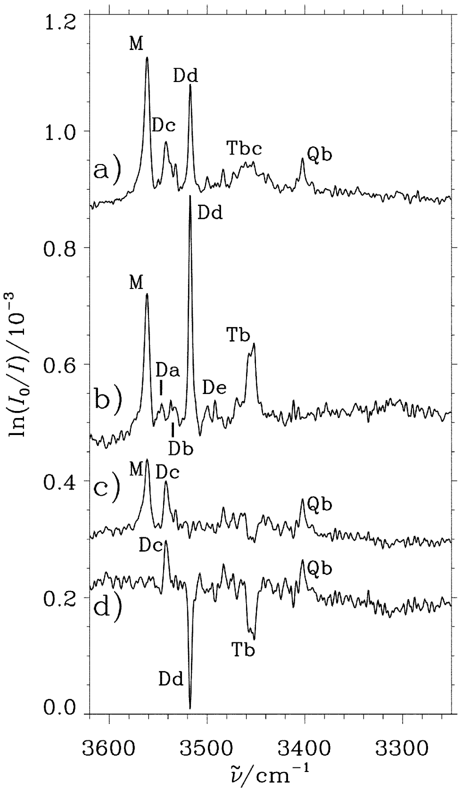

Fig. 5 Chiral recognition in ethyl lactate expansions (~0.05% ELac in He, 0.6 bar, 300 pulses): a) racemate, b) *S*-enantiomer, c) heterochiral part a) − 0.5 × b) and d) difference a) − b) (chirally sensitive fraction, see Fig. 3).

The monomer is red-shifted by 3.5 cm^{-1} in comparison to MLac, indicative of a stronger intramolecular hydrogen bond due to inductive effects. The most prominent band Dd is 2.1 cm^{-1} blue-shifted with respect to Dd in MLac (M-Dd) and has a similar shape. In contrast, E-Da, E-Db and E-De are split. This points at a different dimer conformation than in E-Dd, one in which the ethyl group conformation may play a role in the interaction. The racemic dilution factor for E-Dd (trace a)) is two, again confirming the dimer character of this peak. E-Da and E-Db are superimposed by a heterochiral peak (E-Dc) at 3542 cm^{-1}, similar to M-Dc in the case of MLac.

The E-Tb band equivalent to M-Tb is also split and has homochiral character, giving rise to a racemic dilution factor of about three to four and a negative signal in trace c). The heterochiral partner E-Tc is also split and overlaps with E-Tb, rendering a detailed analysis of the broad racemate spectrum difficult (Tbc).

One important equivalence to MLac is the appearance of a characteristic heterochiral Q cluster, 2.5 cm^{-1} blue-shifted to M-Qb. Pressure dependence suggests a cluster size larger than Tbc. Like E-Dd, the E-Qb band appears to be unsplit, suggesting a minor role of the alkoxy-part in the stabilization of the structure.

In summary, the remarkable analogies between the MLac and ELac spectra support the robustness of the investigated chiral recognition phenomena and the involvement of other than ORR′ groups in the dominant cluster interactions, while subtle differences point at conformational isomerism among the D bands.

3.4 Isopropyl lactate in comparison to ethyl and methyl lactate

Fig. 6 compares the spectra of a) *S*-isopropyl lactate (*S*-ILac), b) *S*-ELac and c) *S*-MLac scaled to a ν_{CH} band strength proportional to the number of C–H bonds, 11 : 9 : 7. As the concentrations of the three compounds differed slightly, conclusions concerning different clustering extent have to be drawn cautiously. The spectrum of S-ILac is remarkably close to that of S-MLac. It exhibits the same band pattern and even comparable intensity ratios in the dimer region. Tb in ILac has a characteristic high-frequency slope in common with MLac. In contrast to ELac, no splittings of Da, Db, De and Tb are observed. This suggests that the corresponding conformers are again symmetric. As shown in Table 4, the ELac-splitting of the Da and Db transitions is accompanied by a relatively large blue-shift. This indicates some minor role of the ethyl ester group on these OH vibrations. On the other hand, the large isopropyl residue does not appear to affect cluster formation noticeably. This supports the existence of intermolecular O–H ··· O=C and O–H ··· O–H building blocks for the cluster structure, whereas the ester group is only involved in secondary interactions. The evolution of the C-bands with increased bulkiness of the ester group suggests that cooperative O–H ··· O–H hydrogen bonding may win over the more isolated O–H ··· O=C connections, which appear to give rise to most of the sharp bands. The more bulky *tert*-butyl lactate is expected to enhance this trend and will be studied in the near future.

Table 4 Band shifts $\Delta\tilde{\nu}$ in cm^{-1} for enantiopure ILac ($\tilde{\nu}_{\mathrm{ILac}} - \tilde{\nu}_{\mathrm{MLac}}$) and ELac ($\tilde{\nu}_{\mathrm{ELac}} - \tilde{\nu}_{\mathrm{MLac}}$) relative to the corresponding MLac band

ELac	$\Delta\tilde{\nu}$	ILac	$\Delta\tilde{\nu}$	rel. to
E-M	−3.5	I-M	−6.0	M-M
E-Da	+7.8, +3.6	I-Da	−6.3	M-Da
E-Db	+8.5, +3.8	I-Db	−1.6	M-Db
E-Dd	+2.1	I-Dd	−2.1	M-Dd
E-De	+3.9, −4.8	I-De	−3.8	M-De
E-Tb	+0.4, −4.1	I-Tb	−4.9	M-Tb
E-Ca	+0.6	I-Cb	−1.1	M-Ca

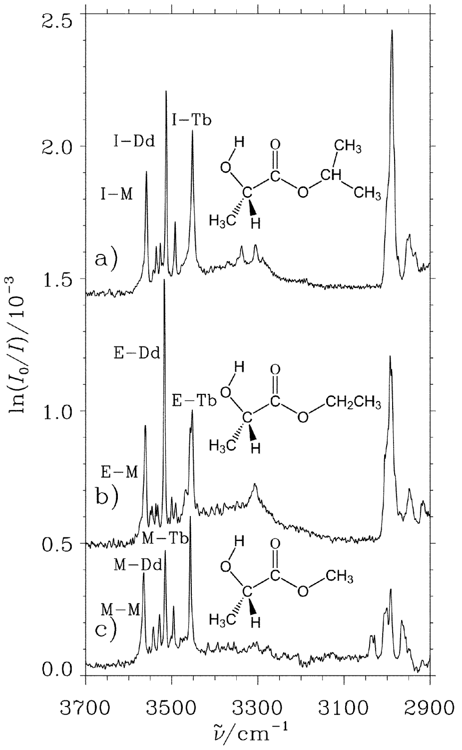

Fig. 6 Comparison of jet spectra of enantiopure a) ILac, b) ELac and c) MLac. For better comparison, spectra are scaled (a) (× 1.2), b) (× 1.5) and c) (× 1)) to a CH-intensity-ratio of 11 : 9 : 7, assuming approximate additivity of the ν_{CH}-absorptions.

3.5 Structural implications

MLac provides insights into an interesting aspect of hydrogen bonding—the competition between intrinsically strong but isolated O–H ··· O=C hydrogen bonds and O–H ··· O–H bonds which only become strong upon cooperative enhancement. One might argue that O–H ··· ORR′ hydrogen bonds should also be discussed in this context, but for the following reasons they can be ruled out:

i) Energetically, the OH group prefers the carbonyl acceptor already in the monomer.[28,29]

ii) We find that analogous spectra of chiral l-methoxy-2-propanol ("decarbonylated" MLac) clusters do not exhibit a prominent Tb-like band.

This reduces the number of different dimer topologies substantially: in analogy to glycidol,[2] symmetric (push–pull) dimers with two reciprocal O–H ··· O=C connections (8-rings) as well as chelating structures in which the O–H group of molecule A is inserted into the internal hydrogen bond of molecule B (5-rings) can be devised. Our ring-nomenclature only counts the number of heavy atoms, as hydrogen bonds tend towards linearity. Fig. 7 illustrates the geometry of such homo- and heterochiral 8- and 5-ring structures. Based on

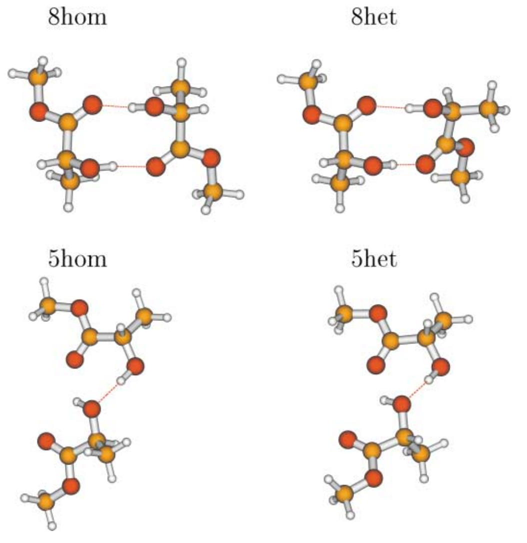

Fig. 7 Schematic illustration of the four most stable MLac dimer structures: homochiral (8hom) and heterochiral (8het) push–pull 8-ring dimers and OH ··· OH ··· O=C chelating homochiral (5hom) and heterochiral (5het) 5-ring dimers.

preliminary *ab initio* calculations, 8-ring dimers are energetically favored over 5-rings for MLac (whereas the opposite seems to be true for the simpler glycolaldehyde).

Substitution of the ester groups should have a minor influence on 8-ring dimers, as they are widely separated. This is in agreement with the dimer absorptions Dc and Dd which are not split in the case of ELac. The high intensity of the homochiral Dd band would result from its thermodynamic stability and the concentration of IR intensity in a single transition. Therefore, an assignment of Dd to 8hom and of Dc to 8het appears likely. Interestingly, the hom/het splitting is ~4 times larger than in glycidol.[2]

The existence of further dimer OH-absorptions implies the presence of 5 ring dimers (Fig. 7). The 5-ring dimers are predicted somewhat higher in energy than 8hom/8het (about 5 kJ mol^{-1} at B3LYP/6-31+G* level and about 10 kJ mol^{-1} at MP2/6-31+G* level), whereas the energetic discrimination between homochiral and heterochiral structures is smaller, on the order of 0 to 3 kJ mol^{-1}.

The non-equivalence of the two MLac units in the 5-rings and the higher flexibility of the chelated unit can cause further conformational isomerism. Secondary interactions between C–H bonds and oxygen acceptor sites different for homo- and heterochiral clusters are conceivable. Thus, the dimer absorptions labeled Da, Db, De and Df are likely to originate in 5-ring dimer structures, but we postpone a detailed assignment to a systematic theoretical analysis.

While the dimer isomerism in lactates shows close analogies to the glycidol case,[2] a major challenge lies in the understanding of aggregation beyond the dimer, where the α-hydroxy carbonyl functionality leads to pronounced chiral discrimination. Exploratory quantum chemical calculations reveal a subtle equilibrium between cooperative O–H ··· O–H and isolated O–H ··· O=C hydrogen bond topologies, and a tendency of the donor O–H group to form bifurcated hydrogen bonds to an O–H and an O=C acceptor, at the same time. Even if these bifurcated structures should not persist as minima at higher levels of theory, they can provide low energy pathways between the limiting single hydrogen bond topologies. We wish to extend the *n*-ring nomenclature used for dimers to this situation. Thus, a MLac trimer can either form a strained 3-ring built from cooperative OH groups, or it can open up in steps of three heavy atoms, replacing a single O–H ··· O(–C–C=O)–H coordination by a O–H ··· O=C–C–O–H sequence. Thus, there are 3-, 6-, 9-, and 12-ring structures for MLac trimers, connected by pathways involving bifurcated hydrogen bonds. Similarly, there are 4-, 7-, 10-, 13-, and 16-ring tetramers. The global minimum of these structures seems to depend quite sensitively on the level of theory, and it cannot be rigorously quantified in terms of ring size, due to the bifurcation. Furthermore, it depends on the substitution of the carbonyl group. Fig. 8 shows the backbones of a 3-ring trimer structure with some 12-ring character and the backbone of a 4-ring tetramer with substantial 16-ring character. Ball-and-stick models viewed perpendicular to and along the C_2 axis is also provided.

The simplest explanation of the Tb band would be that of a strained 3-ring trimer, with a (nearly) degenerate, strongly IR-active band. Comparison to spectra of simple alcohols[24,46,43] shows that Tb falls in the expected frequency range for such a trimer. It is conceivable that the lactate units can arrange more favorably on one side in the homochiral trimer. For the tetramer, alternating up–down arrangements may be more favorable for heterochiral *RSRS* structures.

In summary, we can present the following, most likely assignment hypothesis:

The Tb band is due to a MLac trimer (probably of 3-ring type) and the Q-bands due to a tetramer, both involving substantial OH ··· O= character. This hypothesis is consistent with the pressure dependence and it implies a remarkable preference for homochiral trimers and heterochiral tetramers.

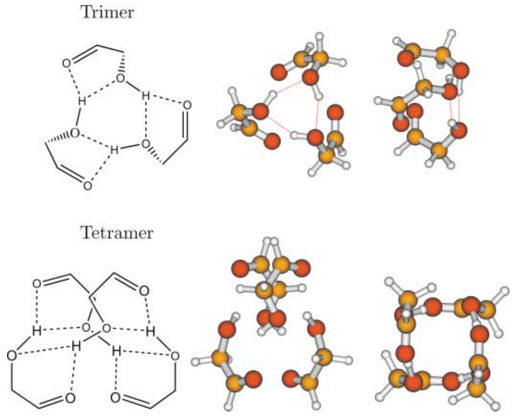

Fig. 8 Schematic illustration of a MLac trimer backbone structure with cooperative OH ··· OH bonds and a tetramer backbone structure which realizes cooperative OH ··· OH bonds and strong OH ··· O=C bonds at the same time. Also shown are two ball-and-stick model views each of the underlying glycolaldehyde trimer and tetramer perpendicular to and along the C_3 axis (trimer) and the C_2 axis (tetramer). By relaxing the hydrogen bonds of the tetramer to OH or C=O, one can make smooth transitions to two more classical conformers without bifurcated hydrogen bonds.

The C-bands are due to homochiral tetramers or larger clusters with dominant OH ··· OH interactions.

In any case, secondary interactions such as C–H ··· O contacts and steric hindrance by α-C methyl groups may be essential for chiral self-recognition. A combined experimental and quantum chemical effort will be required to solve these structural riddles and we have initiated calculations of several conceivable structures.

4 Conclusions

Self-organization of lactates in the gas phase was studied by *ragout*-jet FTIR-spectroscopy. Unprecedented infrared signatures of chiral self-recognition extending to fairly large oligomeric aggregates are observed. Extensive quantum chemical studies and experiments with more direct structural and cluster size information are under way to elucidate this molecular recognition phenomenon in more detail. However, the combination of panoramic spectroscopy, racemic dilution, difference techniques, stagnation pressure dependence, collisional isomerization, argon coating, chemical substitution, and comparison to reference spectra presented in this work already provides some firm conclusions at this stage:

i) Lactate monomers can be prepared in supersonic expansions in a single, internally hydrogen-bonded conformation. The carbonyl group is the favored acceptor group.

ii) Lactate dimers show conformational isomerism, involving at least two, probably more different homochiral and a similar number of heterochiral conformations. Upon argon coating, the spectra of these conformations collapse into a single absorption. The dominating homochiral conformation has a single IR-active OH-stretching band, which is shown not to be sensitive to the ester group. It can be explained by a symmetric, 8-membered ring dimer (see Fig. 7).

iii) A larger oligomer, most likely a trimer, exhibits a strong and sharp OH-stretching band (Tb) for the all-*S* (or all-*R*) diastereomer. This homochiral band persists upon racemic dilution and still accounts for most of the structured IR activity in its spectral neighborhood. The invariance upon Ar-coating suggests that the involved functional groups (O–H and probably C=O) are well protected within the cluster structure. The Tb band, and broader O–H stretching bands (Ca and Cb) typical for cooperative OH ··· OH hydrogen bonds, correlate with a blue-shifted carbonyl stretching band.

iv) Based on stronger pressure scaling, an even larger oligomer (Q) dominates the spectra of racemic mixtures despite statistical competition and must be due to favorable heterochiral aggregation involving the carbonyl groups.

v) Lactates offer a good example for the close competition between intrinsically strong hydrogen bonds to carbonyl groups and cooperatively enhanced hydrogen bonds to hydroxyl groups. It is likely that this competition contributes to the pronounced chiral recognition phenomena.

We do not expect that this specific phenomenon persists in solution, where solvation competes with lactate–lactate interactions. It will still be interesting to study mixed lactate–solvent clusters to observe the solvent influence.

Our next steps towards a microscopic understanding of this remarkable self-organization phenomenon in isolated molecular clusters involve comprehensive quantum chemical calculations, the IR-study of chemically modified molecules such as β-hydroxy esters, α-C modified lactates like methyl glycolate and methyl α-hydroxy-isobutyrate, α-hydroxy-aldehydes and -ketones, extension of the spectral range, coexpansion with simple alcohols and isotope substitution. Several of these investigations are currently under way. Complementary spectroscopic methods such as matrix isolation, IR-UV double resonance, microwave spectroscopy, and size-selected action spectroscopy are also planned in cooperation with other groups. We finally note that α-hydroxy-carboxylic acids, besides their own biological significance, can replace amino acids in so called depsipeptides, thus linking our results to recent spectroscopic studies of β-sheet models in the gas phase.[47]

Acknowledgements

We thank A. Bochenkova, C. Emmeluth, M. Fárník, P. Zielke and M. Weimann for their valuable support and helpful discussions. Cooperation and discussions with A. Zehnacker, F. Lahmani, and R. Fausto have been inspiring. D. Pratt has drawn our attention to Ref. 3, in which molecular handshakes are also invoked to visualize chiral self-recognition. Support by the Fonds der Chemischen Industrie and by the Deutsche Forschungsgemeinschaft via SFB 357 (Molekulare Mechanismen Unimolekularer Prozesse) and the graduate school GRK 782 are gratefully acknowledged.

References

1 E. Fischer, *Chem. Ber.*, 1894, **27**, 2985–2993.
2 N. Borho and M. Suhm, *Phys. Chem. Chem. Phys.*, 2002, **4**, 2721–2732.
3 J. M. Rowland, M. M. Olmstead and P. K. Mascharak, *Inorg. Chem.*, 2002, **41**, 1545–1549.
4 D. P. Craig and D. P. Mellor, *Top. Curr. Chem.*, 1976, **63**, 3–48.
5 L. Salem, X. Chapuisat, G. Segal, P. C. Hiberty, C. Minot, C. Leforestier and P. Sautet, *J. Am. Chem. Soc.*, 1987, **109**, 2887–2894.
6 I. Alkorta and J. Elguero, *J. Am. Chem. Soc.*, 2001, **124**(7), 1488–1493.
7 S. Portmann, A. Inauen, H. P. Lüthi and S. Leutwyler, *J. Chem. Phys.*, 2000, **113**, 9577–9585.
8 I. Paci, J. Dunford and N. M. Cann, *J. Chem. Phys.*, 2003, **118**, 7519–7533.
9 K. Sünkel, W. Hoffmüller and W. Beck, *Z. Naturforsch., B: Chem. Sci.*, 1998, **53**(11), 1365–1368.
10 I. Zahn, K. Polborn and W. Beck, *J. Organomet. Chem.*, 1991, **412**, 397–405.
11 R. G. Cooks, D. Zhang, K. J. Koch, F. C. Gozzo and M. N. Eberlin, *Anal. Chem.*, 2001, **73**, 3646–3655.
12 R. R. Julian, R. Hodyss, B. Kinnear, M. F. Jarrold and J. L. Beauchamp, *J. Phys. Chem. B*, 2002, **106**(6), 1219–1228.
13 M. Quack, *Angew. Chem., Int. Ed.*, 2002, **41**, 4618–4630.
14 M. Iwahashi, H. Matsuzawa, Y. Moroi, M. Czarnecki and Y. Ozaki, *Vib. Spectrosc.*, 1999, **20**, 113–119.
15 A. R. Al-Rabaa, E. Bréhéret, F. Lahmani and A. Zehnacker, *Chem. Phys. Lett.*, 1995, **237**, 480–484.
16 M. Mons, F. Piuzzi, I. Dimicoli, A. Zehnacker and F. Lahmani, *Phys. Chem. Chem. Phys.*, 2000, **2**, 5065–5070.
17 K. Le Barbu, V. Brenner, P. Millié, F. Lahmani and A. Zehnacker-Rentien, *J. Phys. Chem. A*, 1998, **102**, 128–137.
18 A. R. Al-Rabaa, K. Le Barbu, F. Lahmani and A. Zehnacker-Rentien, *J. Photochem. Photobiol. A: Chem.*, 1997, **105**, 277–282.
19 A. Latini, M. Satta, A. Giardini-Guidoni, S. Piccirillo and M. Speranza, *Chem. Eur. J.*, 2000, **6**(6), 1042–1049.
20 A. Filippi, A. Giardini, S. Piccirillo and M. Speranza, *Int. J. Mass Spectrosc.*, 2000, **198**, 137–163.
21 A. Latini, D. Toja, A. Giardini-Guidoni, A. Palleschi, S. Piccirillo and M. Speranza, *Chirality*, 1999, **11**, 376–380.
22 A. K. King and B. Howard, *J. Mol. Spectrosc.*, 2001, **205**, 38–42.
23 A. K. King and B. Howard, *Chem. Phys. Lett.*, 2001, **348**, 343–349.
24 T. Häber, U. Schmitt and M. A. Suhm, *Phys. Chem. Chem. Phys.*, 1999, **1**, 5573–5582.
25 T. Häber, U. Schmitt, C. Emmeluth and M. A. Suhm, *Faraday Discuss.*, 2001, **118**, 331–359.
26 N. Borho, *Diploma thesis*, Inst. f. Phys. Chemie, Göttingen 2001.
27 N. Borho, T. Häber and M. Suhm, *Phys. Chem. Chem. Phys.*, 2001, **3**, 1945–1948.
28 R. Bursi, F. J. Devlin and P. Stephens, *J. Am. Chem. Soc.*, 1990, **112**(25), 9431–9435.
29 D. M. P. Gigante, F. Long, L. A. Bodack, J. M. Evans, J. Kallmerten, L. A. Nafie and T. B. Freedman, *J. Phys. Chem. A*, 1999, **103**(11), 1523–1543.
30 S. Jarmelo and R. Fausto, *J. Mol. Struct.*, 1999, **509**, 183–199.
31 S. Jarmelo, T. M. R. Maria, L. P. Leitão and R. Fausto, *Phys. Chem. Chem. Phys.*, 2000, **2**, 1155–1163.
32 S. Jarmelo, T. M. R. Maria, L. P. Leitão and R. Fausto, *Phys. Chem. Chem. Phys.*, 2001, **3**, 387–392.
33 N. Mori, A. Yuzuru and Y. Tsuzuki, *Bull. Chem. Soc. Jpn.*, 1968, **41**, 1871–1875.
34 G. Cassanas, M. Morssli, E. Fabregue and L. Bardet, *J. Raman Spectrosc.*, 1991, **22**, 409–413.
35 W. M. Coleman and B. M. Gordon, *J. Appl. Spectrosc.*, 1989, **43**(2), 305–310.
36 Y. Nakao, H. Sugeta and Y. Kyogoku, *Chem. Lett.*, 1984, **4**, 623–626.
37 T. B. Freedman, E. Lee and L. A. Nafie, *J. Phys. Chem. A*, 2000, **104**, 3944–3951.
38 T. B. Freedman, E. Lee and T. Zhao, *ACS Symp. Ser.*, 2002, **810**, 65–78.
39 T. Kimura, T. Ozako and S. Tagaki, *Chirality*, 1998, **10**, 722–725.
40 T. Katagiri, C. Yoda, K. Furuhashi, K. Ueki and T. Kubota, *Chem. Lett.*, 1996, **10**(7), 115–116.
41 T. Katagiri and K. Uneyama, *Chem. Lett.*, 2001, **30**, 1330–1331.
42 M. Akazome, T. Takahashi and K. Ogura, *J. Org. Chem.*, 1999, **64**, 2293–2300.
43 D. Zimmermann, T. Häber, H. Schaal and M. A. Suhm, *Mol. Phys.*, 2001, **99**, 413–426.
44 K. Le Barbu, F. Lahmani and A. Zehnacker-Rentien, *J. Phys. Chem. A*, 2002, **106**, 6271–6278.
45 D. Nesbitt, T. Häber and M. A. Suhm, *Faraday Discuss.*, 2001, **118**, 305–309.
46 H. Schaal, T. Häber and M. A. Suhm, *J. Phys. Chem. A*, 2000, **104**, 265–274.
47 M. Gerhards, C. Unterberg and A. Gerlach, *Phys. Chem. Chem. Phys.*, 2002, **4**(22), 5563–5565.